

**Title:** Evolution of Local Microstructures (ELMS): Spatial Instabilities of Coarsening Clusters

545-29

**Principal Investigator:** Martin E. Glicksman, *Rensselaer Polytechnic Institute*

0211-2

**Co-Investigators:** Donald O. Frazier\*, Jan R. Rogers\*, William K. Witherow\*,  
J. Patton Downey\*, Barbara R. Facemire\*  
\*NASA Marshall Space Flight Center, Space Sciences Laboratory

### Introduction

This work examines the diffusional growth of discrete phase particles dispersed within a matrix. Engineering materials are microstructurally heterogeneous, and the details of the microstructure determine how well that material performs in a given application. Critical to the development of designing multiphase microstructures with long-term stability is the process of Ostwald ripening. Ripening, or phase coarsening, is a diffusion-limited process which arises in *polydisperse* multiphase materials. Growth and dissolution occur because fluxes of solute, driven by chemical potential gradients at the interfaces of the dispersed phase material, depend on particle size. The kinetics of these processes are “competitive,” dictating that larger particles grow at the expense of smaller ones, overall leading to an increase of the average particle size. The classical treatment of phase coarsening was done by Todes, Lifshitz, and Slyozov, (TLS)<sup>1,2</sup> in the limit of zero volume fraction,  $V_v$ , of the dispersed phase. Since the publication of TLS theory there have been numerous investigations, many of which sought to describe the kinetic scaling behavior over a range of volume fractions. Some studies in the literature report that the relative increase in coarsening rate at low (but not zero) volume fractions compared to that predicted by TLS is proportional to  $V_v^{1/2}$ , whereas others suggest  $V_v^{1/3}$ . This issue has been resolved recently by simulation studies at low volume fractions in three dimensions by members of the Rensselaer/MSFC team.<sup>3-5</sup>

### Background and Objectives

Our studies of ripening behavior using large-scale numerical simulations suggest that although there are different circumstances which can lead to either scaling law, the most important length scale at low volume fractions is the diffusional analog of the Debye screening length. This screening length places limits on the extent and applicability of a mean-field description and can result in local divergences from mean-field behavior. The numerical simulations we employed exploit the use of a recently developed “snapshot” technique and identify the nature of the coarsening dynamics at various volume fractions. Preliminary results of numerical and experimental investigations, focused on the growth

of finite particle clusters, provide important insight into the nature of the transition between the two scaling regimes. The companion microgravity experiment centers on particle growth within finite clusters and follows the temporal dynamics driving microstructural evolution using holography.

This research effort will extend our preliminary ground-based results and develop a critical microgravity experiment to observe these phenomena in a suitably quiescent environment. Work accomplished to date shows that the critical cross-over between the two scaling regimes ( $V_v^{1/2}$  versus  $V_v^{1/3}$ ) is a function of both the volume fraction, which, intuitively, affects the screening length and the cluster size,  $n$ , where  $n$  is the number of particles comprising the cluster. Specifically, the cross-over occurs at a critical volume fraction for which  $V_v \approx 1/(3n^2)$ . One also expects that the volume fraction itself fluctuates from region-to-region, because the local size and distribution of particles vary. Thus, spatial variances should arise in the local kinetics. One of the scientific objectives of this work is to identify the nature of these microstructural fluctuations. This added level of understanding will be of importance in the development of more predictive models for microstructural evolution in heterogeneous materials.

### Theory

We begin with a discussion of infinitely dilute coarsening systems based on the TLS mean-field solution to coarsening kinetics which is restricted to zero volume fraction of droplet phase. The continuity equation requires that neither nucleation nor coalescence occur, only smooth growth and dissolution:

$$\frac{\partial F}{\partial t} + \frac{\partial}{\partial R} [v(R) \cdot F] = 0 \quad 1.$$

Our approach in this work is to seek to measure and predict  $v(R)$ , the time rate of change of the radius,  $R$ , of a particle, in a given cluster. To obtain  $v(R)$ , certain simplifying assumptions are required:

1. Kinetics are limited by volume diffusion in the matrix, and
2. Diffusion remains quasi-static.

Therefore, the diffusion equation describing the concentration field,  $c(r)$ , in the matrix phase reduces to the Laplace equation:

$$\nabla^2 \varphi = 0, \quad 2.$$

where  $\varphi = (c - c_0)/c_0$ , and  $c_0$  is the equilibrium solubility.

The boundary conditions at the surface of the  $i$ -th particle are specified through the Gibbs-Kelvin local equilibrium relation

$$\varphi_i = \frac{\lambda}{R}, \quad 3.$$

where  $\lambda$  is the capillary length given by,  $\lambda = 2\gamma\Omega/(k_B T)$ , through which all quantities of length are scaled in this mean-field treatment;  $\gamma$  is the droplet-matrix interfacial energy;  $\Omega$  is the atomic volume of the dispersed phase; and  $k_B$  is Boltzmann's constant.

Solution to the Laplace equation, subject to the Gibbs-Kelvin boundary condition, may be written in terms of the Coulomb potential

$$\varphi_i = \left( \frac{z_i e}{4\pi\epsilon} \right) \left( \frac{1}{r} \right), \quad 4.$$

where  $\varphi_i$  is the coulomb potential at a distance  $r$  from an ion of charge  $z_i e$ .

The diffusion potential is, therefore,

$$\varphi(r) = \sum_i \frac{\lambda B_i^{TLS}}{|r - r_i|} + \varphi_\infty. \quad 5.$$

The diffusion analog of electrostatic charge is source/sink strength (volume flux),  $B_i^{TLS}$ , given by

$$B_i^{TLS} = \left( 1 - \frac{R_i}{R^*} \right), \quad 6.$$

where  $R^*$  is the critical radius given by,  $R^* = \lambda / \varphi_\infty$ , and  $\varphi_\infty$  is the background matrix potential, assumed uniform throughout the matrix phase. The zero volume fraction restriction in TLS theory results in the total neglect of direct interactions among particles. A more realistic approach which introduces the influence of volume fraction on coarsening kinetics was employed by Marqusee and Ross.<sup>6</sup> Their approach applies a spatially coarse-grained background diffusion potential, which is the diffusion analog of the electric potential arising from a given charge density,  $\rho$ . An expression for electric potential influenced by  $\rho$  is,

$$\nabla^2 \varphi = -\frac{\rho}{\epsilon_0}. \quad 7.$$

The diffusion analog is, therefore,

$$\nabla^2 \varphi = -4\pi\sigma, \quad 8.$$

where  $\sigma$ , a source/sink density in the matrix space, is analogous to  $\rho$  from electrostatics.  $\sigma$  introduces a coarse-grained local background potential,  $\varphi(\mathbf{r})$ , due to droplets surrounding a coarsening droplet centered at point  $\mathbf{r}$  in the matrix,

$$\varphi(\mathbf{r}) = \sum_i \frac{\lambda B_i}{|\mathbf{r} - \mathbf{r}_i|} \exp(-\kappa \cdot |\mathbf{r} - \mathbf{r}_i|) + \varphi_\infty. \quad 9.$$

The volume flux,  $B_i$ , is now,

$$B_i = \left(1 - \frac{R_i \varphi_\infty}{\lambda}\right) (1 + \kappa R_i) = B_i^{TLs} (1 + \kappa R_i), \quad 10.$$

where  $\kappa$  represents the natural cut-off distance for direct particle interactions via the diffusion field, beyond which the particles are isolated from each other by the intervening two-phase medium.

For droplet clusters comprising finite coarsening systems, one may define physically distinct coarse-grained length scale parameters; among them are:

- the Debye screening radius,  $\Lambda_D \equiv \kappa^{-1}$ .
- the average droplet radius in the cluster,  $\Lambda_R \approx \langle R \rangle$ ,

therefore,  $\Lambda_D = [4\pi N_V \langle R \rangle]^{-1/2}$ . As in electrostatics, for large  $\Lambda_D$  (sparse particle density), the screened potential approaches the unscreened potential.

- the extent of the total coarsening system,  $\Lambda_{tot}$ , is defined for a “spherical cluster” by

$$\Lambda_{tot} = \left(\frac{4\pi}{3}\right)^{-1/3} \left(\frac{n}{N_V}\right)^{1/3}, \quad 11.$$

where  $n$  is the total number of particles remaining at a given time, and for  $\Lambda_D \geq \Lambda_{tot}$ , screening is not a factor.

One can now relate the time-rate of change of radius,

$$v(R_i) = - \frac{2\lambda D c_o \Omega}{R_i^2} B_i, \quad 12.$$

whereby  $B_i$  is now representative of the volume flux of a droplet in a finite coarsening cluster. The experimental parameters for determining the time-rate of change of each

droplet within a given cluster are accessible through physicochemical measurement and holography.

### Experiment

Experimental objectives of ELMS are:

- to measure  $v(R_i)$  of each droplet cluster by using holography
- to determine, in a mixed-dimensional system (3-*D* droplets undergoing 2-*D* diffusion), the existence, if any, of spatial instabilities in microstructural homogeneity due to a heretofore undefined “screening length”
- to verify in a fully 3-*D* system in microgravity the TLS coarsening rate deviation dependence on local volume fractions for global volume fractions  $\leq 1\%$ , where the volume fraction for a finite coarsening cluster is,

$$V_v = \frac{\sum_{i=1}^n (4/3)\pi R_i^3}{(4/3)\Lambda_{tot}^3} . \quad 13.$$

The experimental approach is comprised of ground-based work to extend prior mixed-dimensional studies and a flight experiment to study finite coarsening kinetics in three dimensions.

#### **A. Ground-based experiment**

The ground-based experimental study of diffusional coarsening will proceed in a liquid-liquid two-phase system. Ideally, one performs the experiment at an isopycnic point to maximize reduction of gravity-driven convective disturbances. This would allow observations over the long times required to investigate diffusional coarsening. A holographic technique has been instrumental in prior work on this subject and will continue to be the primary method to study both the influence of local environmental conditions on individual droplet size histories and measurements of global averages. Most of the ground-based coarsening data will be collected during two-dimensional diffusion of three-dimensional droplets attached to a glass surface (mixed-dimensional case).<sup>4,5</sup>

Ground-based studies will proceed as follows:

- Prepare droplet distributions for sparse and densely populated clusters for finite coarsening systems undergoing 2-*D* diffusion;

- Configure a pre-programmed x-y translator with predetermined droplet positions in tandem with a sharp tool for scoring pinpoint defects onto high-quality, pristine cell walls. This should induce heterogeneous nucleation at desired positions;
- Fabricate an optimal cell for achieving predictable cluster size and number distributions, and perform experiments;
- Study temporal correlation of droplet size and number distribution for mixed-dimensional coarsening.

## B. Flight Experiment

The space-based coarsening study requires long-duration, quality microgravity to prevent phase separation via Stokes settling. In this instance, there is no wall attachment to prevent sedimentation, so establishing microgravity conditions is an imperative. As the estimated time of the experiment is almost four months, a Space Station facility will ultimately be required.

In order to understand the need for quality microgravity, it is helpful to examine the velocity of a 100 $\mu$ m diameter droplet (the largest size anticipated) at a temperature near the isopycnic point. The Hadamard-Rybczynski relation provides the velocity of droplets,

$$V_s = \frac{2}{3} \frac{\left[ r^2 (\rho_2 - \rho_1) \left( \frac{\eta_2}{\eta_1} + 1 \right) a \right]}{[3\eta_2 + 2\eta_1]}, \quad 14.$$

where  $\rho_2 - \rho_1$  is the mass density difference between the droplet and matrix phases,  $\eta_1$  is the viscosity of the matrix fluid, and  $\eta_2$  is the viscosity of the droplet phase fluid. The Hadamard-Rybczynski relation is valid provided that the droplet surface is clean, and the Reynolds number,  $Re = \rho |V_s| r / \eta_1$ , is small compared to unity. Droplets are assumed to remain spherical. Assuming the use of a succinonitrile-water system, and using a succinonitrile-rich droplet phase with a 0.1K deviation from the isopycnic temperature,  $\Delta\rho \approx 3.85 \times 10^{-5} \text{ g/cm}^3$ . Such a deviation could occur from either experimental uncertainties in the isopycnic set point and the temperature measurement system, as well as from cycling or drift caused by the temperature control system. The magnitude of the velocity of such a droplet at  $10^{-4}g$  is  $1 \times 10^{-4} \text{ mm/hr}$ . In 1-g, the same droplet would fall 1mm in 1hr, and would reach the bottom of the test cell before noticeable ripening had occurred. The dispersion would become rapidly depleted of larger ripening droplets. The relative position of the droplets would also vary significantly in time. It would not be possible to explore local microstructural effects from diffusion, because the droplet population would be altered more rapidly by sedimentation effects. This and other factors, such as distortion around the diffusion field, would obscure the kinetics. These factors impose the imperative for microgravity investigation of three-dimensional coarsening kinetics and observation of evolution of microstructure.

Preparation for microgravity studies will begin by assessing two approaches for droplet dispersion:

1. Jet break-up in microgravity to control the distribution of droplets in each cluster.

From Tomitika, the Rayleigh stability criterion,  $q$ , is expressed as,

$$q = \frac{\gamma}{2\eta_2} (1 - x_d^2) \Phi \left( x_d, \frac{\eta_2}{\eta_1} \right), \quad 15.$$

where  $\eta_1$  and  $\eta_2$  are viscosities of the fluids;  $\gamma$  is the interfacial tension;  $R$  is radius of liquid cylinder; and  $x_d = 2\pi R/\lambda_d$ .  $\lambda_d$  is the wavelength of disturbance caused by, e.g., vibrations or nozzle roughness. For appropriate jet velocity and nozzle wetting characteristics, the average droplet size in a cluster is approximately twice the nozzle diameter. For  $q < 0$ , disturbances damp out; for  $q = 0$ , disturbances remain stable, resulting in oscillating waves; for  $q > 0$ , disturbances become capillary waves which lead to liquid cylinder breakup [pressure limits drop size].

**Table 1. Results from prototype: distribution of butyl–benzoate droplets in water<sup>7</sup>**

$\underline{d_N}(\mu\text{m})$	$\langle d \rangle(\mu\text{m})$	$\sigma(\mu\text{m})$	$\langle d \rangle/\underline{d_N}$
77	149	$\pm 66$	1.9
153	284	$\pm 130$	1.9
203	348	$\pm 190$	1.7

$\underline{d_N}$  is the nozzle diameter;  $\langle d \rangle$  is the average cluster droplet diameter;  $\sigma$  is the standard deviation within the cluster from average cluster droplet diameter.

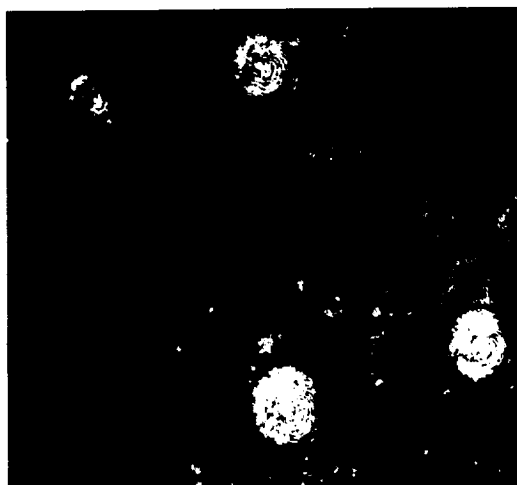
2. Site saturation method [Nucleation of Crystals from Solution (NCS)]<sup>8</sup> for forming droplet clusters by quench.

Finally, holographic imaging is the optical tool selected for observing these phenomena. Figure 1 contains a sequence of holograms during the mixed-dimensional coarsening of succinonitrile-water. Figure 2 represents maps of local diffusion fields derived from spatial and size distributions of all droplets observed in the corresponding holograms of Figure 1 using monopole approximations. Clearly, holography provides more data than does conventional optical imaging techniques. A reconstructed hologram is amenable to various optical characterization techniques, e.g., *in situ* microscopy, and interferometry. An especially important aspect of the experimental study includes determining the extent of modifications required to allow incorporation of holography within the operating envelope of the millikelvin thermostat (MITH) hardware.

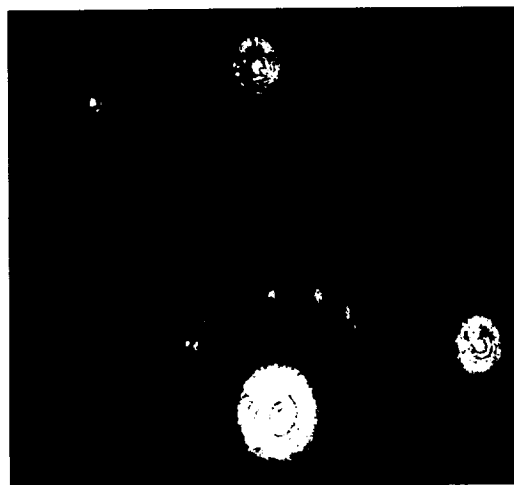
## References

1. O.M. Todes, *J. Phys. Chem (Sov)* **20**, 629 (1946).
2. I.M. Lifshitz and V.V. Slyozov, *J. Phys. Chem. Solids* **19**, 35 (1961).
3. V.E. Fradkov, M.E. Glicksman, S.P. Marsh, *Phys. Rev. E* **53**(3), 3925 (1996).
4. J.R. Rogers, J.P. Downey, W.K. Witherow, B.R. Facemire, D.O. Frazier, V.E. Fradkov, S.S. Mani, and M.E. Glicksman, *J. Electronic Mat.* **23**(10), 999 (1994).
5. V.E. Fradkov, S.S. Mani, M.E. Glicksman, J.R. Rogers, J.P. Downey, W.K. Witherow, B.R. Facemire, and D.O. Frazier, *J. Electronic Mat.* **23**(10), 1007 (1994).
6. J.A. Marqusee and J. Ross, *J. Chem. Phys.* **80**, 536 (1984).
7. J.R. Rogers, Ph.D. Dissertation, University of Colorado, 1992
8. R.L. Kroes, D.A. Reiss, and S.L. Lehoczky, *Microgravity Sci. Technol.* VIII/1 52-55, (1995).

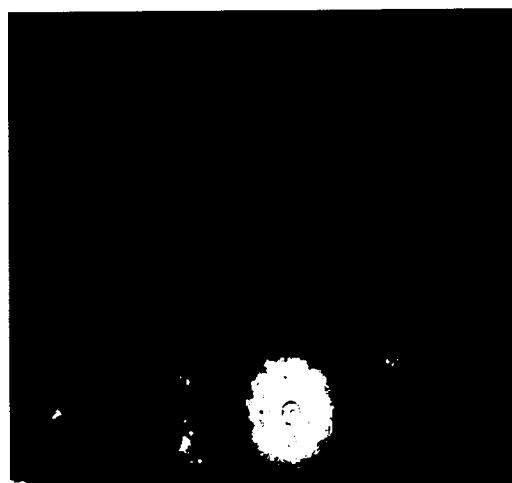
**Holograms of mixed-dimensional coarsening of succinonitrile-water system in pyrex cells: discrete phase is succinonitrile rich.**



**Hologram 100**



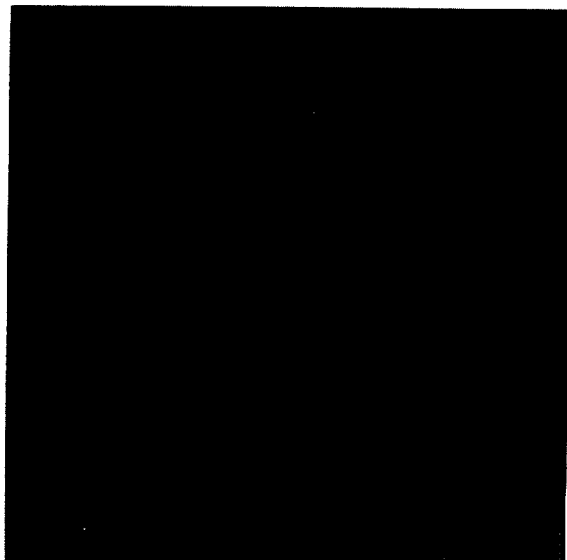
**Hologram 129**



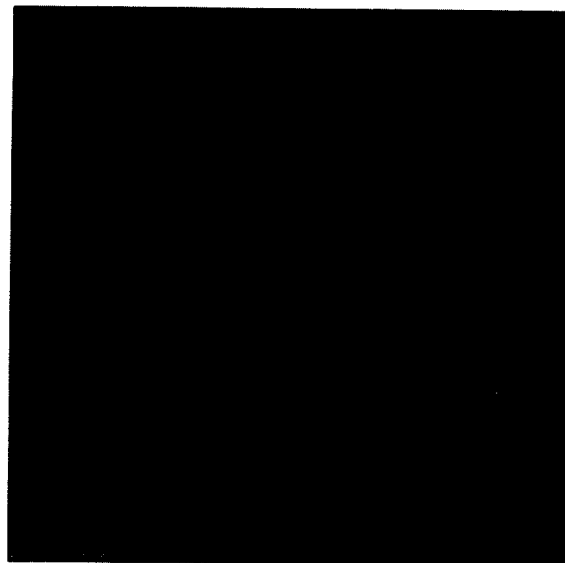
**Hologram 151**

Figure 1.

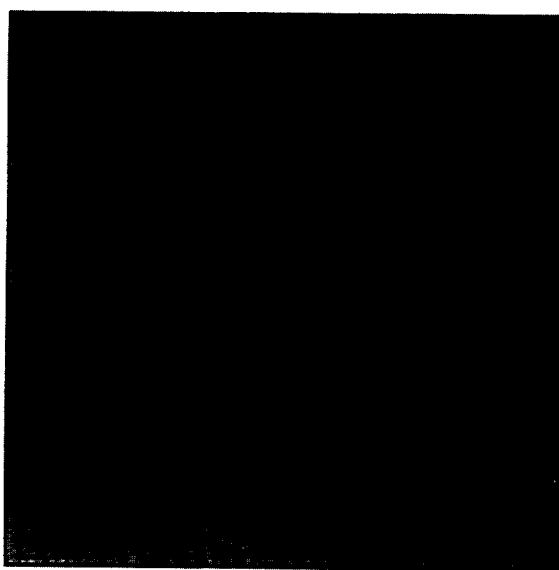
Holographic data for mixed-dimensional coarsening, with mapping of local diffusion fields using monopole approximations. Black circles show particle sizes, shades of blue indicate areas of solute depletion, whereas shades of red show enrichment.



Hologram 100



Hologram 129



Hologram 151

Figure 2.